

Antennal Mechanosensors Mediate Flight Control in Moths

Sanjay P. Sane,^{1*} Alexandre Dieudonné,¹ Mark A. Willis,² Thomas L. Daniel¹

Flying insects have evolved sophisticated sensory capabilities to achieve rapid course control during aerial maneuvers. Among two-winged insects such as houseflies and their relatives, the hind wings are modified into club-shaped, mechanosensory halteres, which detect Coriolis forces and thereby mediate flight stability during maneuvers. Here, we show that mechanosensory input from the antennae serves a similar role during flight in hawk moths, which are four-winged insects. The antennae of flying moths vibrate and experience Coriolis forces during aerial maneuvers. The antennal vibrations are transduced by individual units of Johnston's organs at the base of their antennae in a frequency range characteristic of the Coriolis input. Reduction of the mechanical input to Johnston's organs by removing the antennal flagellum of these moths severely disrupted their flight stability, but reattachment of the flagellum restored their flight control. The antennae thus play a crucial role in maintaining flight stability of moths.

When performing complex three-dimensional maneuvers, it is necessary for flying organisms to assess their self-motion and to respond to unintended perturbations with a rapid modulation of their wing motion (1, 2). Among winged insects, diverse strategies have evolved to resolve this problem. Insects, such as dragonflies, that

typically operate under brightly lit conditions may accomplish course control primarily using visual input to modulate their motor output (3). However, for insects flying under low-light conditions, the longer latency of visual processing (4) means that it may not be possible for such insects to rely entirely on their visual systems to assess self-motion to generate rapid maneuvers.

In Diptera, rapid acquisition of self-motion information is accomplished by halteres, club-shaped sensory structures that are evolutionarily derived from the hind wings and oscillate at wing beat frequency (5). The halteres and their underlying sensory neurons transduce information about pitch, roll, and yaw maneuvers to the central nervous system (5–9). Although a single muscle actively powers haltere motion with a fixed phase relation to the wing, the overall dynamics of the haltere motion are dictated primarily by its natural frequency (5). During rotational maneuvers, Coriolis (or gyroscopic) forces on the halteres cause a lateral deviation in their plane of motion (5, 9). Because the planes of oscillation of the two halteres are nonorthogonal, this system can unambiguously distinguish between pitch, roll, or yaw rotations (9). Although the haltere system has received much attention because it addresses the problem of rapid course control in Dipteran flight, fewer studies have examined how non-Dipteran in-

¹Department of Biology, University of Washington, Seattle, WA 98195, USA. ²Department of Biology, Case Western Reserve University, Cleveland, OH 44106, USA.

*To whom correspondence should be addressed. E-mail: sane@u.washington.edu

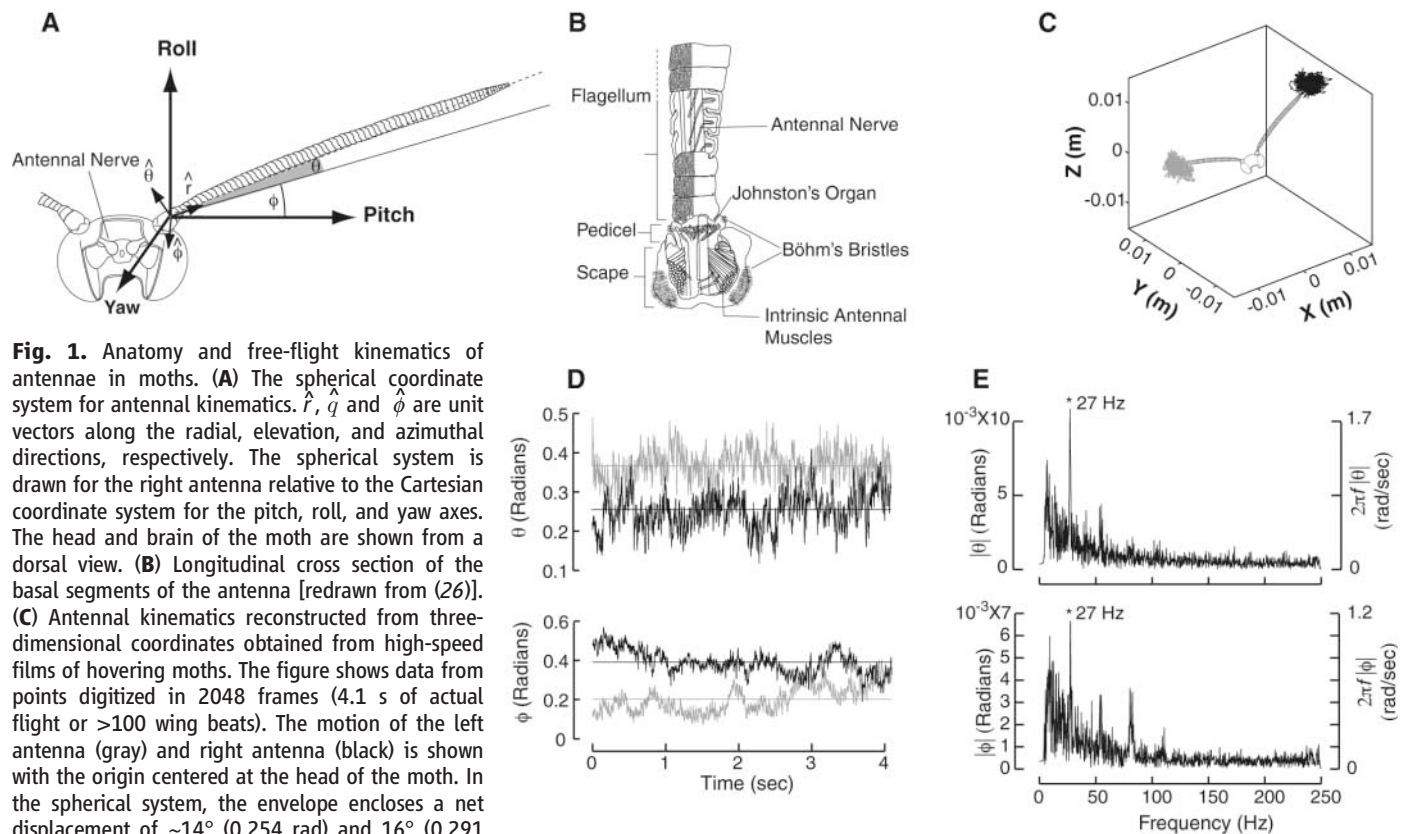


Fig. 1. Anatomy and free-flight kinematics of antennae in moths. **(A)** The spherical coordinate system for antennal kinematics. \hat{r} , \hat{q} and $\hat{\phi}$ are unit vectors along the radial, elevation, and azimuthal directions, respectively. The spherical system is drawn for the right antenna relative to the Cartesian coordinate system for the pitch, roll, and yaw axes. The head and brain of the moth are shown from a dorsal view. **(B)** Longitudinal cross section of the basal segments of the antenna [redrawn from (26)]. **(C)** Antennal kinematics reconstructed from three-dimensional coordinates obtained from high-speed films of hovering moths. The figure shows data from points digitized in 2048 frames (4.1 s of actual flight or >100 wing beats). The motion of the left antenna (gray) and right antenna (black) is shown with the origin centered at the head of the moth. In the spherical system, the envelope encloses a net displacement of $\sim 14^\circ$ (0.254 rad) and 16° (0.291 rad) along the θ angle, and $\sim 19^\circ$ (0.331 rad) and 22° (0.379 rad) along the ϕ angle, for the left and right antenna, respectively. **(D)** Antennal motions along the orthogonal θ and ϕ angles. For the left antenna (gray), the pitch axis points in the opposite direction. Hence, the value of ϕ is shown after subtracting π from its actual value relative to the right-handed pitch-roll-yaw coordinate system. **(E)** Fourier

decomposition of the mean offset removed movement of the right antenna for the θ , ϕ angles. The sharp peaks indicate that antennae vibrate at a wing beat frequency of 27 Hz (asterisk). The amplitude of the vibration was conservatively estimated to be 1.4° and 0.8° along the θ and ϕ angles, respectively.

sects (10, 11), especially those flying under the poorly lit conditions that make visual stabilization difficult, might achieve similar maneuvering feats.

Our investigations suggest that in the crepuscular hawk moth *Manduca sexta*, which is four-winged and thus lacks halteres, the antennal mechanosensory system mediates flight stability using a mechanism similar to the halteres in Diptera. All winged insects, including moths and butterflies, possess a pair of annulated antennae (Fig. 1, A and B). Two sets of antennal mechanosensors are present on the basal antennal segments called the scape and pedicel (Fig. 1B). One set, called the Böhm's bristles, is present as fields of sensory hairs on the scape and the pedicel. In hawk moths, these fields are roughly opposite each other on each segment and roughly orthogonal to each other between two segments. The second set, called the Johnston's organ, is composed of circumferentially arranged mechanosensory stretch receptors called scolopidia. Each scolopidium is innervated by a bipolar neuron

(12), which sends its axon down the length of the antennal nerve into the brain of the moth. The head-scape and scape-pedicel joints each consist of extrinsic (not shown) and intrinsic muscles, respectively (Fig. 1B), which drive all active antennal movements.

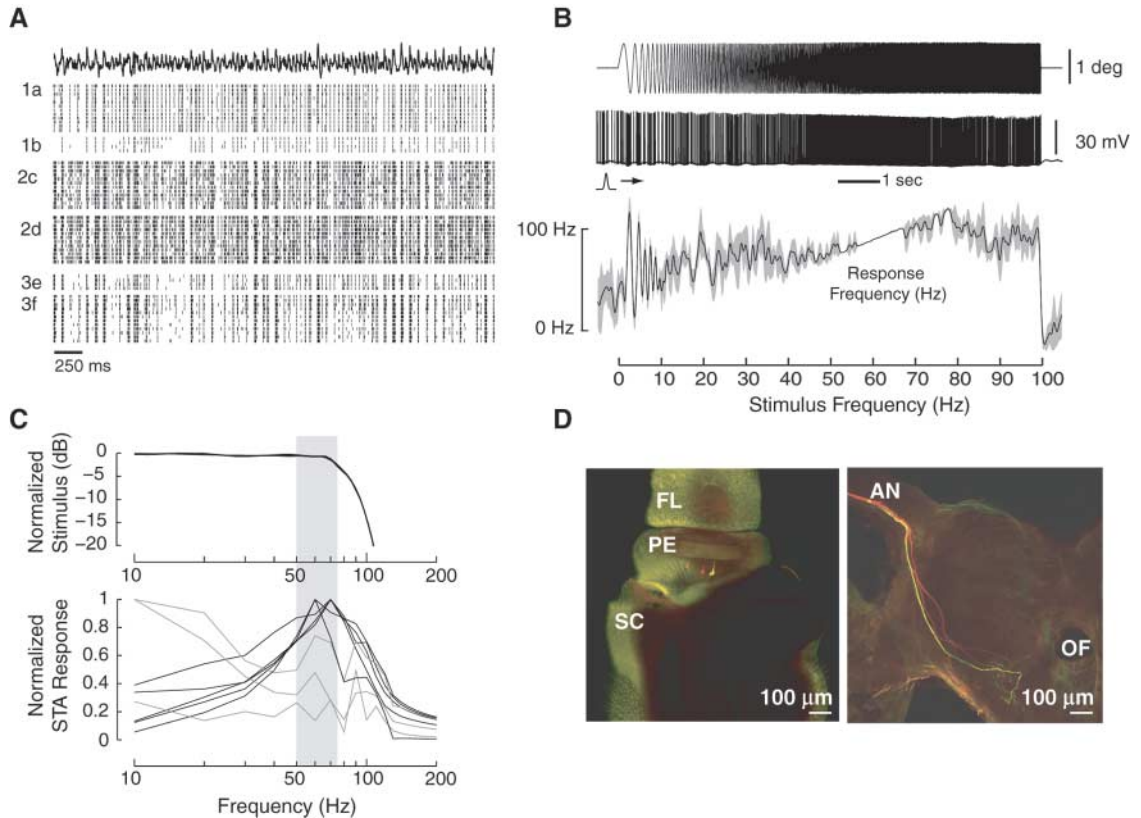
The antennal anatomy of *M. sexta* is common to most free-living insects (12). Data from silk moths (13) and butterflies (14) suggest that the Böhm's bristles encode the gross changes in antennal position, whereas the Johnston's organ responds to small, high-frequency motions of the antenna (15) such as vibrations due to sound or air flow (12, 15, 16). Several reports have described the possible mechanosensory function of antennae as airflow sensors (14, 17–22). We measured the antennal motion of freely hovering *M. sexta* using high-speed videography (500 frames per second; Fig. 1, C and D) [(23), section S1] and found that like some other Lepidopterans [e.g., the tortoiseshell butterfly, *Aglais urticae* (22)], they hold their antennae at relatively constant interantennal angles (Fig. 1C)

[(23), section S1]. About this fixed position, the antennae undergo small-amplitude vibrations (Fig. 1D) with relatively little change in the antennal length [(23), section S1]. The motions of the left (gray) and right (black) antenna are roughly in phase, suggesting symmetry of movement of the two antennae. Fourier transforms of these vibrations revealed prominent peaks at wing beat frequency (27 Hz; Fig. 1E). Thus, the net mechanical stimulus experienced by the antenna contains a periodic self-generated component.

The cross product of the angular velocity of body rotations and linear velocity of the moth's antennal vibrations results in Coriolis torques on the antenna. For hovering and near-hovering conditions, estimates of the torques due to Coriolis and aerodynamic forces are of the same orders of magnitude, and thus Coriolis forces also represent an important component of the net mechanical stimulus to the antennae [(23), section S2]. Like the halteres in Diptera (5, 9), Coriolis torques thus cause lateral deflections of the antennae at either wing beat frequency

Fig. 2. Neurophysiology of mechanosensory neurons.

(A) Spiking response of antennal mechanosensors. Raster plots of the spiking response of scolopidial neurons from the Johnston's organ in response to the "natural" stimulus in Fig. 1C. Peak antennal displacement ranged from 1° to 2.5° (three moths, six cells). The numbers in the side bar represent individual moths and letters represent individual cells. The trials consisted of repetitions of the 4-s-long "natural" stimulus repeated 4 or 12 times. **(B)** Response of an antennal scolopidium to a constant-amplitude frequency sweep from 0 to 100 Hz. A mechanical lever attached to the flagellum delivered a constant-amplitude (~1.5° peak-to-peak) frequency sweep (0 to 100 Hz, top panel) motion to the pedicel-flagellar joint. The corresponding spike response (middle panel) was measured



from the axon of a scolopidial neuron and is shown as the Gaussian-convolved firing rate (black, bottom panel). The gray band enveloping this curve shows the standard deviation of the Gaussian-convolved firing rate. The width of the narrow Gaussian window is 500 ms with a standard deviation of 31.6 ms. **(C)** Stimulus-response curves for scolopidial neurons. Shown are the BLGN stimulus (top panel) and Fourier transforms for the mean spike-triggered average (STA) stimulus for eight scolopidial cells from three moths (bottom panel). The input stimulus is smoothed by the use of Welch's method and normalized with respect to maximum amplitude. The response displayed as a Fourier transform of spike-triggered average for each neuron is also normalized as a ratio of its maximum

response. Of the eight neurons shown here, five (black lines) show sharp peaks between ~50 and 75 Hz and three (gray lines) show greater responses at lower frequency. **(D)** Anatomy of the scolopidial neurons. Scolopidia were filled with Alexa Fluor 568 (red) or Lucifer Yellow (yellow) dyes (left panel, four neurons). The soma of these bipolar neurons is situated in the joint between flagellum (FL) and pedicel (PE). SC denotes scape. The recordings shown in (B) were taken from the one of the neurons filled with Lucifer Yellow. Length of the scale bar is 100 μm. The neurons send their projections ipsilaterally via the antennal nerve (AN) into the antennal mechanosensory and motor center (AMMC) in the deutocerebrum of the moth, on either side of the esophageal foramen (OF) (right panel).

or twice wing beat frequency during maneuvers [(23), section S3; figs. S2 to S4]. Are the mechanosensors in basal segments of the antennae sufficiently sensitive for detecting the Coriolis forces on a vibrating antenna? To answer this question, we recorded intracellularly from the axons of individual scolopidial neurons in the Johnston's organ while subjecting the flagellum to controlled vibrations using a mechanical lever system [(23), section S4; fig. S5]. We observed strong stimulus-correlated activity of scolopidial neurons in response to mechanical stimuli in the amplitude and frequency range of natural motion (Fig. 2A). The alignment of the spikes in these records over multiple trials shows that scolopidial neurons are sensitive to small-amplitude ($\sim 1^\circ$) angular deflections in the flagella-pedicel joint. In response to constant-amplitude frequency sweep (0 to 100 Hz) motion of the antenna, the scolopidial neurons tightly phase-locked with the stimulus in a narrow frequency range of ~ 50 to 70 Hz. In this range, their firing rate increases linearly with the stimulus frequency (Fig. 2B). The 50- to 70-Hz window also corresponds to twice the typical range of wing beat frequency in *M. sexta* (20 to 30 Hz) (24) and is the expected frequency range for the Coriolis input [(23), section S3].

To rigorously characterize the frequency-response properties of the underlying sensory

apparatus, we vibrated the flagellum using a band limited Gaussian noise (BLGN) waveform in a frequency window of ~ 0 to 100 Hz with a -3 -dB roll-off at ~ 85 Hz (Fig. 2C, top panel). We measured the intracellular spike responses of the scolopidial neurons and determined the pre-spike stimulus within a 100-ms time window before the occurrence of each spike of the time record. A Fourier transform of this spike-triggered average (STA) was used to estimate the stimulus frequency most likely to generate action potentials in the scolopidial neurons (25). A subset of the recorded scolopidial neurons (five out of eight; Fig. 2C, bottom panel) showed sharp response peaks in the frequency range of ~ 50 to 75 Hz and is thus capable of encoding Coriolis-driven lateral motions of the antennae during aerial maneuvers. To determine the location and projection patterns of these neurons, we filled them with fluorescent dyes after recording. In all cases, the images showed bipolar neurons innervating the scolopidia in the Johnston's organ and arborized ipsilaterally into the antennal mechanosensory and motor center (AMMC) in the brain, the main site of integration of the mechanosensory signal from the antennal deflections (Fig. 2D) (26, 27).

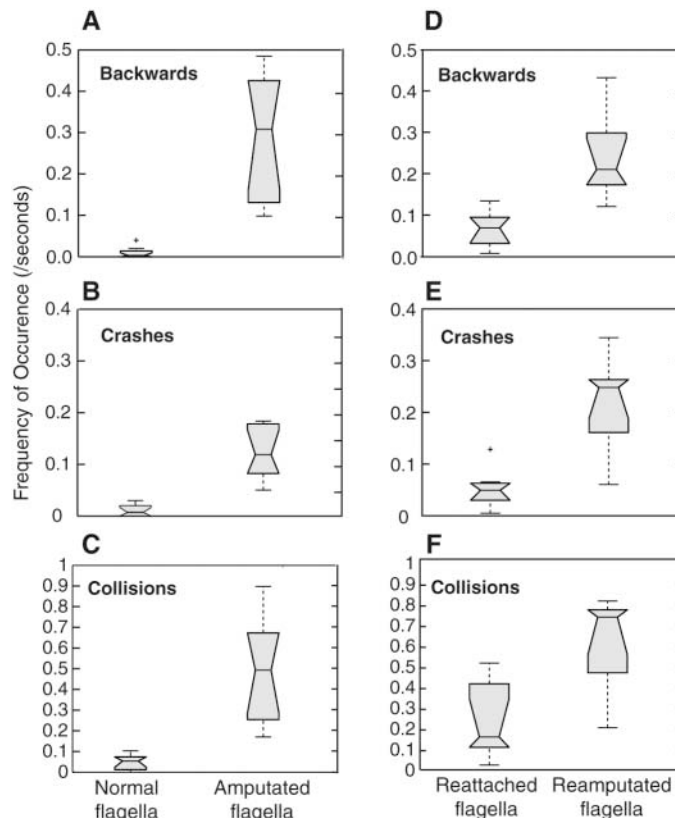
Thus, our results suggest that the antennae of *M. sexta* (and also perhaps other Lepidopterans) are capable of detecting the Coriolis forces gen-

erated during turning maneuvers and may be involved in flight stabilization. Does a reduction of the mechanosensory input from the antenna affect flight performance? To answer this question, we performed experiments manipulating the mechanical loading on the Johnston's organs and measured the free-flight performance of the moths via videography under low-light conditions [(23), section S5]. This study consisted of two experiments. First, we compared the flight performance of moths with intact antennae (normally loaded Johnston's organs) to that of moths with their flagella surgically removed (unloaded Johnston's organs). Second, to control other sensory influences of an intact flagellum, we compared the performance of individuals whose flagella were removed and reattached (reloaded Johnston's organs) to that of the same individuals after removing the flagella again (unloaded Johnston's organs). In all cases, the basal mechanosensory apparatus was left intact and only the flagellum was cut within a few (< 10) annuli from the base. This ensured that the mechanical stimulus due to vibrating antennae was substantially reduced.

To analyze the effect of the flagellar amputation on flight performance, we counted the occurrences of three types of behavior in each flight sequence: (i) collisions with the wall, (ii) crashes to the floor, and (iii) incidence of backward flight (typically spanning the entire width of the flight chamber) [(23), sections S5 to S7]. Moths with amputated flagella could take flight, but had a significantly higher frequency of backward flight than intact moths [(23), section S7; Fig. 3A]. These moths also crashed [(23), section S7; Fig. 3B] and collided [(23), section S7; Fig. 3C] with the walls significantly more frequently than moths with intact flagella ($P < 0.02$). These results indicate that intact flagella are necessary for stable flight in *M. sexta*.

The flagella of most insect antennae are multisensory structures bearing odor, humidity, and temperature sensors in addition to mechanosensory bristles along the flagellum (12). Thus, in moths with amputated flagella, not only is the normal mechanical loading of Johnston's organs disrupted, but these various sensory cues are also eliminated. Which of these functions is primarily responsible for the lack of flight stability in moths with amputated flagella? To answer this question, we reattached the flagella to the basal antennal segments of the moths with glue and compared their flight performance with moths without flagella [(23), section S5]. Moths with reattached flagella were able to substantially regain flight control [(23), section S8]. In contrast, moths with no flagella flew backward significantly more often (Fig. 3D), crashed to the ground more often (Fig. 3E), and collided with walls more frequently (Fig. 3F). Because the surgical removal and reattachment of the antennal flagella with Super Glue required cold anesthesia, these moths were analyzed separately from the earlier flagella-amputated group. Moths

Fig. 3. Free-flight behavior of moths with and without antennal mechanosensory input. Data from behavioral experiments are represented as notched, whisker plots. The bottom and top of the box show lower and upper quartile values, respectively. The horizontal black line within the box represents the median for each category. Whiskers include the most extreme data value up to 1.5 times the interquartile range. The outlier points beyond this range are shown by the + symbol. Nonoverlapping notches indicate different medians at the 5% significance level. Top row shows data for backward flight, middle row for crashes, and bottom row for collisions. The left column (A to C) shows behavior of moths with intact antennae versus amputated flagella (Wilcoxon signed rank test, $P = 0.002$). The right column (D to F) shows behavior of moths with reattached flagella versus reamputated flagella (Wilcoxon signed rank test, $P = 0.0156$).



with reattached flagella receive no input from any sensory neurons on the flagella because their antennal nerve is severed during the removal and reattachment of flagella. Thus, the restoration of normal mechanical loading of Johnston's organs is sufficient for recovery of flight control in moths with reattached flagella.

In summary, our study of antennal vibrations in freely flying moths and subsequent estimates of the mechanical forces on vibrating antennae suggest that antennae experience strong Coriolis forces during aerial maneuvers. Our neurophysiological data indicate that antennal mechanosensors are tuned within the frequency range of these forces. The antennectomy experiments show that normal loading of the mechanosensors in the base of the antennae, probably the Johnston's organ, is critical for flight stability. Moths without flagella can take flight but cannot stably hover or execute controlled maneuvers. However, moths with reattached flagella regain flight control. Therefore, we propose that the antennae together with the mechanosensors in their bases are necessary for flight stability in *M. sexta*, similar to halteres in flies. These data provide a mechanism to explain previous observations that antennectomy compromises flight in other Lepidoptera (21). Moreover, it is possible that the end knobs on the antennae of certain Lepidoptera (e.g., butterflies)

and other insects (e.g., owl flies) function as a means of increasing the sensitivity to Coriolis forces by enhancing antennal vibrations during flight. Thus, these studies offer an insight into the non-haltere-mediated mechanisms for course control in flying insects and may be useful to studies of insect flight, as well as to recent efforts toward designing robotic insects.

References and Sections

1. T. S. Collett, M. F. Land, *J. Comp. Physiol.* **99**, 1 (1975).
2. H. Wagner, *Philos. Trans. R. Soc. London B Biol. Sci.* **312**, 553 (1986).
3. R. M. Olberg, *J. Comp. Physiol.* **141**, 327 (1981).
4. E. J. Warrant, *Vision Res.* **39**, 1611 (1999).
5. J. Pringle, *Philos. Trans. R. Soc. London B Biol. Sci.* **233**, 347 (1948).
6. G. Nalbach, R. Hengstenberg, *J. Comp. Physiol.* **175**, 695 (1994).
7. W. P. Chan, F. Prete, M. H. Dickinson, *Science* **280**, 289 (1998).
8. M. H. Dickinson, *Philos. Trans. R. Soc. London B Biol. Sci.* **354**, 903 (1999).
9. G. Nalbach, *J. Comp. Physiol.* **173**, 293 (1993).
10. W. Pix, G. Nalbach, J. Zeil, *Naturwissenschaften* **80**, 371 (1993).
11. V. B. Wigglesworth, *Nature* **157**, 655 (1946).
12. D. Schneider, *Annu. Rev. Entomol.* **9**, 103 (1964).
13. D. Schneider, K. E. Kaissling, *Zool. Jahrb. Abt. Anat. Ontog. Tiere* **75**, 287 (1956).
14. M. Niehaus, M. Gewecke, *Zoomorphologie* **91**, 19 (1978).
15. L. H. Field, T. Matheson, *Adv. Insect Physiol.* **27**, 86 (1998).
16. D. Robert, M. C. Gopfert, *J. Insect Physiol.* **48**, 189 (2002).
17. M. Gewecke, in *Experimental Analysis of Insect Behaviour*, L. B. Browne, Ed. (Springer, Berlin, Heidelberg, New York, 1974), pp. 100–113.
18. M. Gewecke, *Nature* **225**, 1263 (1970).
19. H. G. Heinzel, M. Gewecke, *J. Comp. Physiol.* **161**, 671 (1987).
20. M. Gewecke, H. G. Heinzel, *J. Comp. Physiol.* **139**, 357 (1980).
21. M. Niehaus, *J. Comp. Physiol.* **145**, 257 (1981).
22. M. Gewecke, M. Niehaus, *J. Comp. Physiol.* **145**, 249 (1981).
23. Materials and methods are available as supporting material on Science Online.
24. S. P. Sane, N. P. Jacobson, *J. Exp. Biol.* **209**, 43 (2006).
25. P. Dayan, L. F. Abbott, *Theoretical Neuroscience: Computational and Mathematical Modeling of Neural Systems* (MIT Press, Cambridge, MA, 2005).
26. P. Kloppenburg, S. M. Camazine, X. J. Sun, P. Randolph, J. G. Hildebrand, *Cell Tissue Res.* **287**, 425 (1997).
27. J. S. Vande Berg, *J. Morphol.* **133**, 439 (1971).
28. We gratefully acknowledge M. Tu for sharing high-speed videos of hovering moths; T. Hedrick for help with digitization; A. Hinterwirth and A. Mountcastle for assistance with behavior experiments; Som and Suma Chilukuri for their support; and an anonymous referee for useful feedback. Support was provided by an NSF Inter-Disciplinary Informatics Grant (S.P.S.) and the Office of Naval Research (T.L.D. and M.A.W.).

Supporting Online Material

www.sciencemag.org/cgi/content/full/315/5813/863/DC1

Materials and Methods

Figs. S1 to S5

Movies S1 to S3

8 August 2006; accepted 8 January 2007

10.1126/science.1133598